ACI STRUCTURAL JOURNAL TECHNICAL PAPER

Title No. 116-S39

Investigation into Resilience of Precast Concrete Floors against Progressive Collapse

by Kai Qian and Bing Li

The casualties and economic loss in historic events have revealed that progressive collapse performance of buildings has to be evaluated in structural design to prevent such disastrous events. Integrity and resilience are important characteristics for buildings to prevent total collapse or disproportionate collapse once an unpredictable terrorism event unfortunately occurs. Compared to the extensive studies on behavior of cast-in-place reinforced concrete (RC) buildings for progressive collapse resistance, there is less research on precast concrete (PC) buildings to mitigate progressive collapse. Thus, in this study, three one-story, two-bay large-scale frame-floor subassemblies (one RC and two PC) are tested under pushdown loading regime to investigate the effect of PC floor units and transverse beams on progressive collapse resilience of PC moment-resisting frames. It is found that the PC beams and slab systems could provide substantial compressive arch action and compressive membrane action, similar to the cast-in-place RC buildings. However, as PC slabs are discontinuous, insignificant tensile membrane action is able to develop in PC slab systems and the ultimate load capacity in enormous deformation stage is mainly attributed to the catenary action developed in PC beams.

Keywords: load-resisting mechanism; monolithic connection; precast concrete; progressive collapse; resilience.

INTRODUCTION

With the increase of terrorist activities in recent years, the possibility of buildings subjected to unexpected load scenarios is a real one. One of the consequences is the building structures would lose one or several columns due to bomber attack, which will enlarge the shear force and bending moments of the structural components in the immediate vicinity of the damaged area. In such scenarios, conventional designed buildings, especially gravity designed buildings, may not be able to resist the amplified bending moment and shear force purely relied on the flexural action, and progress to propagation of the damage. This type of collapse is defined as progressive collapse or disproportionate collapse. To ensure that the remaining part of the building is able to generate an alternate bridging system, secondary load-resisting mechanisms (compressive arch action, catenary action, compressive membrane action, and tensile membrane action) are preferred. However, the efficiency of the load-resisting mechanisms is related to the integrity and ductility of the building directly. To study the secondary load-resisting mechanisms of buildings in mitigating progressive collapse, researchers have conducted several numerical and experimental investigations[1-14] in the past decade. However, a majority of the current studies are dedicated to cast-in-place reinforced concrete (RC) buildings. Few studies, especially experimental works, have been focused on precast concrete (PC) buildings resisting progressive collapse.[15] It is known that the integrity of PC buildings may be inferior to the cast-in-place RC buildings depending on the construction methods and connection types.[16] Extensive studies on PC buildings in resisting seismic loading have indicated that PC buildings with monotonic beam-column connections may achieve similar seismic resistance as RC buildings.[17] Thus, PC buildings with monotonic connections are frequently used in developed countries[18] due to their fast construction speed, ease in quality control, low labor power, and site spacing requirements. However, there is still uncertainty regarding the resilience of PC buildings with monotonic connections to resist progressive collapse as the lateral seismic loading scenario is quite dissimilar with the vertical gravity load redistribution after some columns are lost accidentally. Thus, to evaluate the resilience of PC frames with PC slab system, three one-story, two-bay large-scaled frame-floor subassemblages (one cast-in-place RC and two PC) with size of 5475 x 2175 mm (215 x 86 in.) were fabricated and tested at Nanyang Technological University (NTU), Singapore, in this study.

RESEARCH SIGNIFICANCE

The primary objective of this paper is to experimentally evaluate the resilience of PC buildings to resist progressive collapse. The significance of the test lies in the fact that such large-sized tests of integrated three-dimensional (3-D) frame-floor assemblies, which are more representative of the complex loading transfer mechanisms in real PC frame buildings, are rare in available literature. Moreover, the test results may benefit researchers and design engineers to apprehend the possible load resisting mechanisms in PC buildings to mitigate progressive collapse. The outcomes from this study may provide strong evidence to establish more convincing design guidelines, as few provisions are addressed for PC structures to mitigate progressive collapse in current design guidelines due to little related experimental data.

EXPERIMENTAL PROGRAM

Test specimens

Three specimens (RC1, PC1, and PC2) are designed and tested in this study. Among the specimens, RC1 is cast-in-

ACI Structural Journal, V. 116, No. 2, March 2019.

MS No. S-2018-085.R1, doi: 10.14359/51710878, was received March 15, 2018, and reviewed under Institute publication policies.

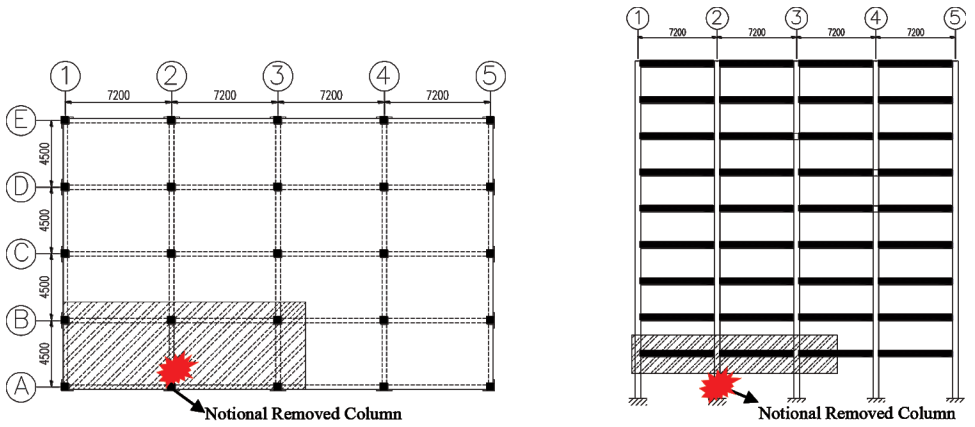

(a) (b)

Fig. 1—Dimensions of prototype building: (a) plan view; and (b) elevation view. (Note: Units in mm; 1 mm = 0.0393 in.)

Table 1—Specimen properties

Test ID	Beam cross section		Column cross section, mm, (in.)	Beam reinforcement ratio				Topping layer		Precast concrete slab
				Longitudinal beam		Transverse beam				
	Longitudinal, mm (in.)	Transverse mm, (in.)		Neg.	Posi.	Neg.	Posi.	Thickness mm, (in.)	Welded wire reinforcement, mm	
RC1	170 x 100 (6.7 x 3.9)	155 x 100 (6.1 x 3.93)	170 x 170 (6.7 x 6.7)	1.3%	1.0%	1.5%	1.1%	N/A	N/A	N/A
PC1	170 x 100 (6.7 x 3.9)	155 x 100 (6.1 x 3.9)	170 x 170 (6.7 x 6.7)	1.3%	1.0%	1.5%	1.1%	20 (0.8)	R3@150	Along tran. direction
PC2	170 x 100 (6.7 x 3.9)	155 x 100 (6.1 x 3.9)	170 x 170 (6.7 x 6.7)	1.3%	1.0%	1.5%	1.1%	20 (0.8)	R3@150	Along long. direction

Note: 1 mm = 0.393 in.

place and taken as a control specimen for reference. PC1 and PC2 are two other PC specimens with comparable dimensions and reinforcement details as RC1. As shown in Fig. 1, the prototype building corresponding to RC1 is gravity designed with design span of 7.2 and 4.5 m (283.5 and 177 in.) in longitudinal and transverse directions, respectively. The cross section of the beam in longitudinal and transverse directions is 300 x 510 and 300 x 465 mm (12 x 20 and 12 x 18 in.), respectively. The average live load (LL) is 2.5 kPa (0.36 psi) and the dead load (DL) due to self-weights is 6.1 kPa (0.88 psi). As shown in Table 1, only one-third-scaled specimens are designed and tested given the space limitation in the laboratory. The reinforcements are proportioned down by keeping a similar reinforcement ratio. The curtailments of beam longitudinal reinforcement are also proportioned down. Figure 2 shows the dimensions and reinforcement details of RC1. It can be seen that only a single story with two panels is extracted from the building for testing as it is assumed that the lost column A2 is an exterior column, which is just nearby the corner column A1. As tabulated in Table 1 and shown in Fig. 2, the beam span in longitudinal and transverse directions is 2.4 m (94 in.) and 1.5 m (59 in.), respectively. And the cross section of the longitudinal and transverse beams is 100 x 170 mm (3.9 x 6.7 in.) and 100 x 155 mm (3.9 x 6.1 in.), respectively. In addition, the column is 170 mm (6.7 in.) square. As shown in Fig. 3, for PC1, similar dimensions and reinforcement details as RC1 are designed. However, the beam, column, and hollow core slab are precast individually before casting the topping layer. To provide a seat for precast beams, a corbel with size of 80 x 120 mm (3.1 x 4.7 in.) is cast incorporating with precast column. Similarly, for providing seats to precast slabs, lodges with size of 50 x 80 mm (2.0 x 3.1 in.) are cast with PC beams. The beam longitudinal reinforcements are continuous by weld connection in the joint zone. The thickness of the PC slab is 65 mm (2.6 in.) but the topping layer has additional thickness of 20 mm (0.8 in.). As shown in Fig. 3, for the precast slab, R3 with spacing of 70 mm (2.8 in.) is reinforced in longitudinal direction while R3 with spacing of 140 mm (5.5 in.) is reinforced in the transverse direction as distributed reinforcements. Furthermore, the welded wire reinforcement of R3 with spacing of 150 mm (5.9 in.) is reinforced in the topping layer. For PC2, comparing to PC1, the only difference is the direction of precast slabs. In PC2, the PC slab is laid along the longitudinal direction with length of 2.3 m (90.6 in.). It should be noted that the diameter and spacing of the hollows in PC slab are identical for PC1 and PC2. The precast specimens were built in several stages, which took more than 2 months. First, the partial height beams, columns, and precast concrete hollow core slabs were cast. Then, these precast members were then erected in the laboratory, and the beam-column joint and topping layer was cast. Figure 4 displays the schematic view of the assemblies in laboratory.

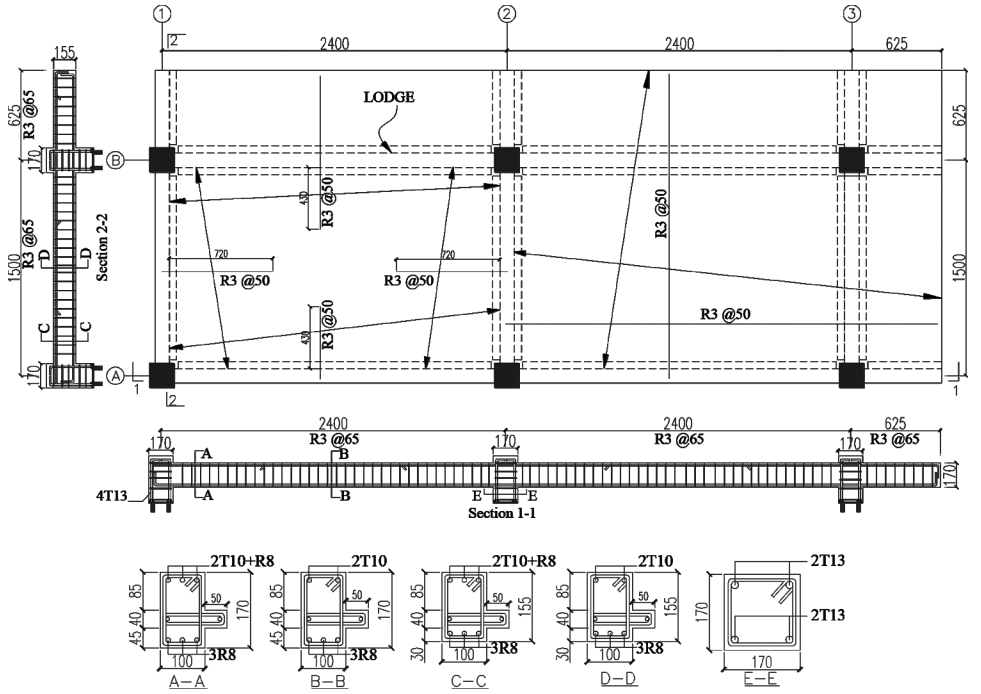

Fig. 2—Details of control Specimen RC1. (Note: Units in mm; 1 mm = 0.0393 in.; T is deformed reinforcing bar; R is plain reinforcing bar.)

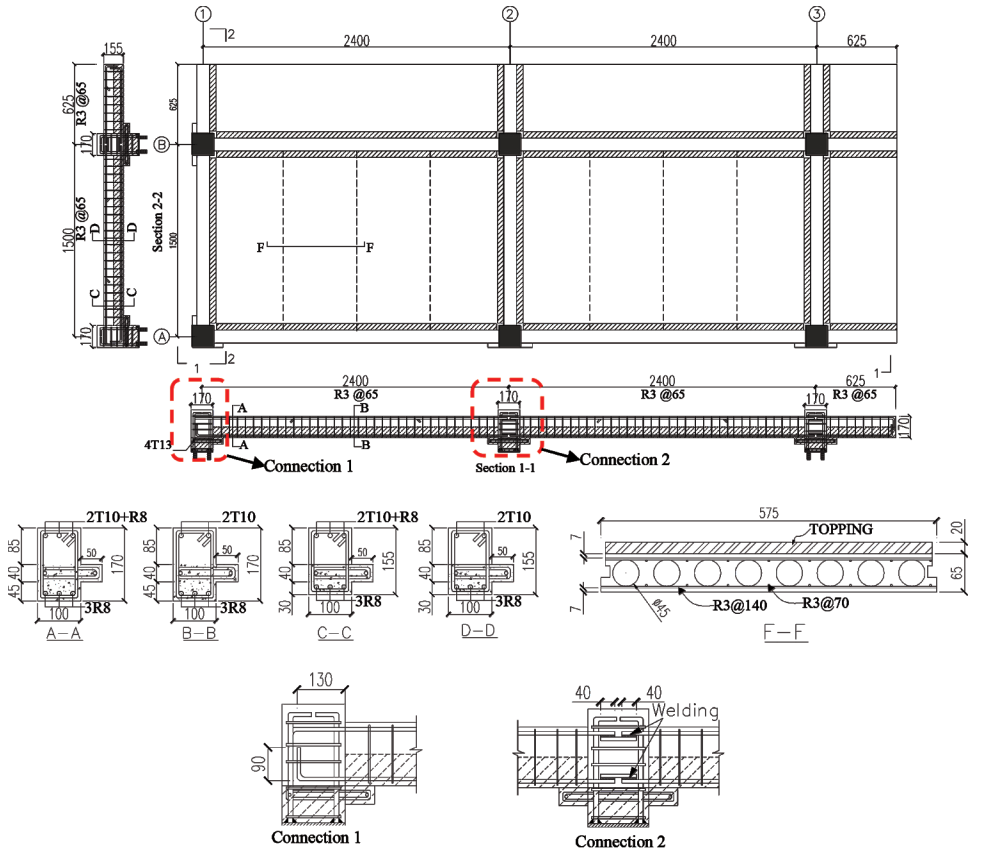

Fig. 3—Details of precast Specimens PC1. (Note: Units in mm; 1 mm = 0.0393 in.; T is deformed reinforcing bar; R is plain reinforcing bar.)

Material properties

At 28 days after cast, the measured concrete compressive strength of RC1 is 32.2 MPa (4.7 ksi). The concrete compressive strength of precast hollow core slab, precast beam, and column is 33.3 and 34.6 MPa (4.8 and 5.0 ksi) for PC1 and PC2, respectively. However, the concrete compressive strength of the topping layer in PC1 and PC2 are 31.9 and 30.5 MPa (4.6 and 4.4 ksi), respectively. The yield strength

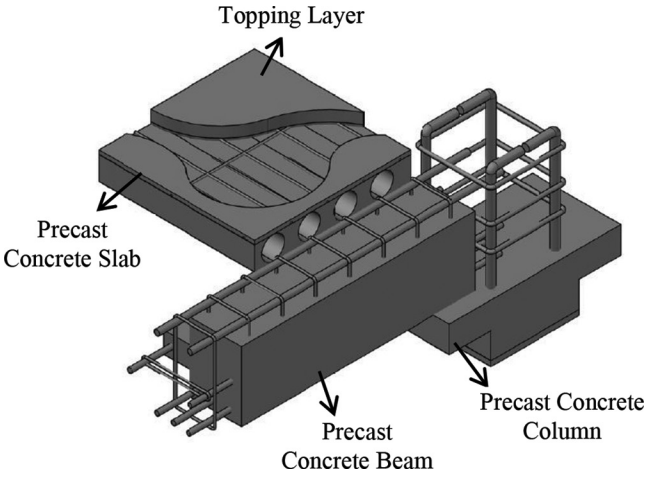

Fig. 4—Schematic view of assemblies in laboratory.

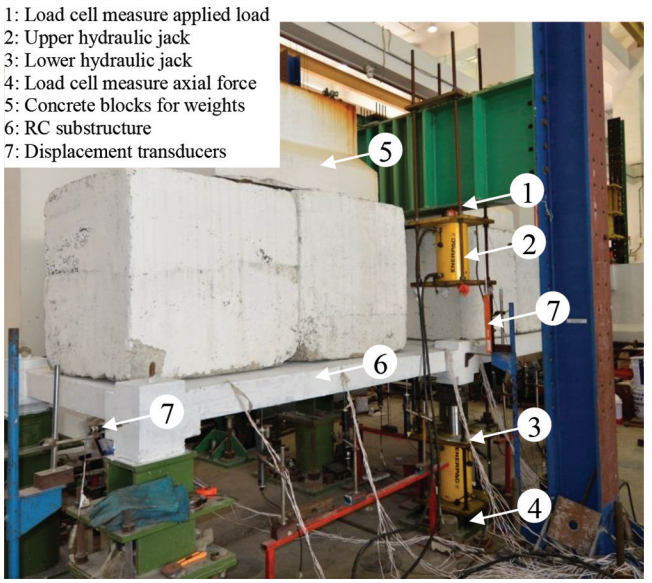

Fig. 5—Overview of precast specimen in position ready for testing.

of R3, R8, T10, and T13 are 431, 504, 531, and 556 MPa (62.4, 19.8, 77.0, and 80.6 ksi), respectively. However, the ultimate strength of R3, R8, T10, and T13 are 511, 589, 614, and 643 MPa (74.0, 85.4, 89.0, and 93.2 ksi), respectively.

Test setup and procedure

Figure 5 depicts the experimental setup of typical precast Specimen PC1. The specimen is fixed on the steel supports by pre-installed bolts in RC columns, except column A2. For Column A2, a hydraulic jack (Item 3 in Fig. 5) is installed beneath it to simulate it is intact before testing. Then, the special combined concrete blocks (Item 5 in Fig. 5) with total weight of 12 tonnes (13.2 tons) are applyied on the top surface to simulate the design service load with dynamic increase factor (DIF) of 2.0. When all concrete blocks were applied symmetrically, the stroke of the lower hydraulic jack (Item 3 in Fig. 5) began to retract to simulate the removal of the column gradually. If the specimen could reach stability after the stroke of the lower jack was detached from the column stub completely, the upper hydraulic jack (Item 2 in Fig. 5) began to apply additional axial force on

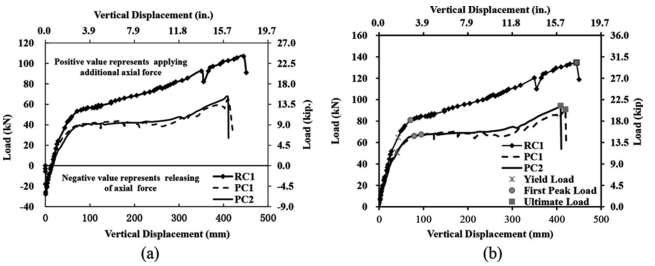

Fig. 6—Load-displacement curve of test specimens: (a) before shifting; and (b) after shifting.

the lost Column A2 to evaluate the ultimate behavior of the specimens.

Instrumentation

Extensive measurement devices were installed both internally and externally to monitor the behavior of test specimens. A load cell (Item 4 in Fig. 5) was used to monitor the varying of axial force in lower hydraulic jack (Item 3 in Fig. 5). Another load cell (Item 1 in Fig. 5) was installed to measure the applied additional force. A series of linear variable displacement transducers (LVDTs) were placed horizontally or vertically. The horizontally installed LVDT is used to monitor the horizontal movement of column A1 during tests, while vertically installed LVDTs were placed at various locations below the beam or slab to measure the vertical displacement distribution and deflection shape. A series of strain gauges were attached on the reinforcements to monitor the varying of strains in the specimens.

EXPERIMENTAL RESULTS

Global behavior and failure modes

Control Specimen RC1—The measured load-displacement curve of RC1 is shown in Fig. 6(a) and the key results are tabulated in Table 2. The negative value represents the phase of releasing axial force while the positive value means applying additional axial force on the lost column. As mentioned previously, the concrete blocks with total weights approximately 12 tonnes (13.2 tons) are slowly applied on the top surface of the slab before test. The maximum axial force of –28 kN (–6.3 kip) is measured in the load cell (Item 4 in Fig. 5) just beneath the lower jack, as shown in Fig. 6(a). To simulate the gradual removal of the column, the stroke of the lower hydraulic jack begins to retract progressively. Accompanying the retraction of the stroke, Column A2 begins to move downward while the axial force in the lower jack begins to decrease. To demonstrate the load-resisting capacities and comparison of the load-resisting functions, the load-displacement curves are shifted from the minimum load point to origin of the coordinate system, as shown in Fig. 6(b). For example, the point (–0.9 in., –28 kN [–0.03 in., –6.3 kip]) is shifted to (0, 0) for RC1. It should be noted that the load presented afterward is the value after shifting. As shown in Fig. 6(b), when the axial force increased to 20 kN (4.5 kip), cracks were observed in the interior beam and slab nearby Column B2. Further retracting the stroke to detach it from the bottom of Column A2, the measured vertical displacement at Column A2 is 13 mm

Table 2—Test results

Test	Displacement at critical status, mm (in.)				Load capacity at critical status, kN (kip)		
	FRAF	First yield	First peak load	Ultimate deformation	First yield	First peak load	Ultimate load
RC1	13 (0.5)	44 (1.7)	71 (2.8)	451 (17.8)	64 (14.4)	81 (18.2)	135 (30.3)
PC1	15 (0.6)	39 (1.5)	95 (3.7)	420 (16.6)	51 (11.5)	68 (15.3)	91 (20.4)
PC2	16 (0.6)	41 (1.6)	79 (3.1)	409 (16.1)	50 (11.2)	66 (14.8)	94 (21.1)
PC1/RC1	1.15	0.89	1.33	0.93	0.80	0.84	0.67
PC2/RC1	1.23	0.93	1.11	0.91	0.78	0.81	0.70

Notes: FRAF is full release of axial force; 1 mm = 0.393 in.; 1 kN = 0.225 kip.

(0.5 in.) and no reinforcement is yielded. Detaching from A2 represents the clear removal of the column. The re-stabilization of the specimen would mean the control specimen could survive a sudden removal of Column A2 (the magnitude of weights has considered the dynamic effects due to sudden column loss). After that, the stroke of upper jack (Item 2 in Fig. 5) begins to protrude out to apply additional concentrated force at Column A2. When the vertical displacement at Column A2 reaches 44 mm (1.7 in.), reinforcement yielding is observed in longitudinal reinforcement of beam B2-A2. Further pushing the vertical displacement to 71 mm (2.8 in.), the first peak load (FPL) of 81 kN (18.2 kip) is obtained. At this stage, the cracks in the beams and slabs become wider and concrete crushing is observed in the beam end near to Column B2. Further increasing the displacement, the load resistance begins to re-ascend. When the displacement reaches 193 mm (7.6 in.), concrete spalling becomes severe in the joint of Column B2. The ultimate load capacity of 135 kN (30.3 kip) is measured at a vertical displacement of 451 mm (17.8 in.). The failure mode of Control Specimen RC1 is shown in Fig. 7. It is seen that extensive cracks formed in both top and bottom of the slab. Shear failure occurred in the joint zone of corner Column A1 due to significant axial force developed in the Beam A1-A3 in large deformation stage. However, no palpable shear crack occurred in the interior Joint A3 due to additional horizontal constraints from the extending part of the slab. Reinforcing bar fracture is observed in the beam end near to Column A3. Severe crushing concrete is observed in the beam ends near to A1, B2, and A3. Moreover, severe spalling of concrete is observed in the slab nearby B2.

Precast Specimen PC1—Similar to RC1, the measured axial force in the lower jack is approximately –27 kN (–6.1 kip) after applying the weights of 12 tonnes (13.2 tons). As shown in Fig. 6(b), when the load increased to 18 kN (4.0 kip) based on the shifted curve, the interface between the precast slab and interior beams B1-B3 showed some sign of minor opening. When the load increased to 27 kN (6.1 kip), which means the lower jack detached from the Column A2 completely, the vertical displacement is measured to 15 mm (0.6 in.). Cracks were also apparent at the interface between precast concrete slab and the transverse beams A1-B1 and A3-B3. Then, the upper jack begins to push the specimen further downward. The yielding of beam longitudinal reinforcement is achieved when the applied load reached 52 kN (11.7 kip), which is approximately 80% of that of RC1. At this loading point, cracks are not only observed in the top surface but also in the bottom surface of the slab. The FPL of 68 kN (15.3 kip), which is approximately 84% of that of RC1, is obtained at the vertical displacement of 95 mm (3.7 in.). The ultimate load capacity of 91 kN (20.5 kip), which is approximately 67% of that in RC1, is obtained at a vertical displacement of 420 mm (16.5 in.). Figure 8 shows the failure modes of PC1. As shown in Fig. 8(a), a large opening with maximum width of 15 mm (0.6 in.) is observed in the interface between precast slabs and Beam B1-B3. From the bottom view, although the cracks in the precast slabs are continual, differential vertical and horizontal movement is observed in between the precast slabs due to relatively rotation occurring at the interfaces. Similar to RC1, plastic hinges also occurred in the beam end near to A1, A3, and B2. Concrete spalling is more severe in the plastic hinge near to column B2 than that near to A1 and A3. In addition, shear failure is also observed in the corner joint (Column A1). However, it is less severe than that in RC1 as less tensile force developed in the stage of catenary action and tensile membrane action.

Precast Specimen PC2—After shifting, the load-displacement curve of PC2 is illustrated in Fig. 6(b). When the lower jack detached Column A2 completely (the load increased to 27 kN [6.1 kip]), the vertical displacement measured to 16 mm (0.6 in.). The yield load capacity of 50 kN (11.2 kip) is obtained at a displacement of 41 mm (1.6 in.). Moreover, the FPL of 66 kN (14.8 kip) is reached at a displacement of 79 mm (3.1 in.). Compared to PC1, similar ultimate load capacity of 94 kN (21.1 kip) is achieved at a displacement of 409 mm (16.1 in.). Figure 9 demonstrates the failure mode of PC2. As shown in Fig. 9, opening with maximum width of 25 mm (1.0 in.) occurred in the interface between precast slab and interior Beam B1-B3. Compared to PC1, the distribution of cracks in the slab is much finer. From the bottom view, openings are also observed in the interfaces between the precast slabs and in the interfaces between the precast slab and surrounding beam, although the cracks are continual. However, from the top view, the integrity of the slab is very well and thus, the risk of falling down of precast slabs is low for tested PC1 and PC2.

Horizontal movement of Column A1

As revealed previously, horizontal movement of Column A1 is monitored during tests to quantify the possible load resisting mechanism developed in the specimens. For Specimen RC1, as shown in Fig. 10, outward movement is observed first. The maximum outward movement is

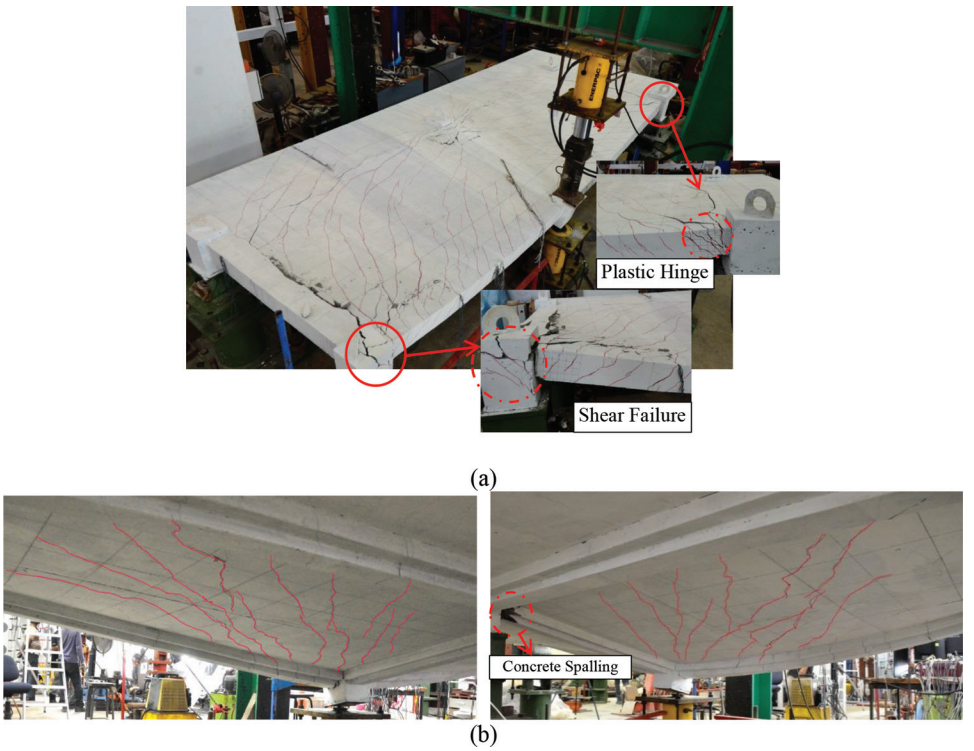

Fig. 7—Failure mode of Specimen RC1: (a) top view; and (b) bottom view.

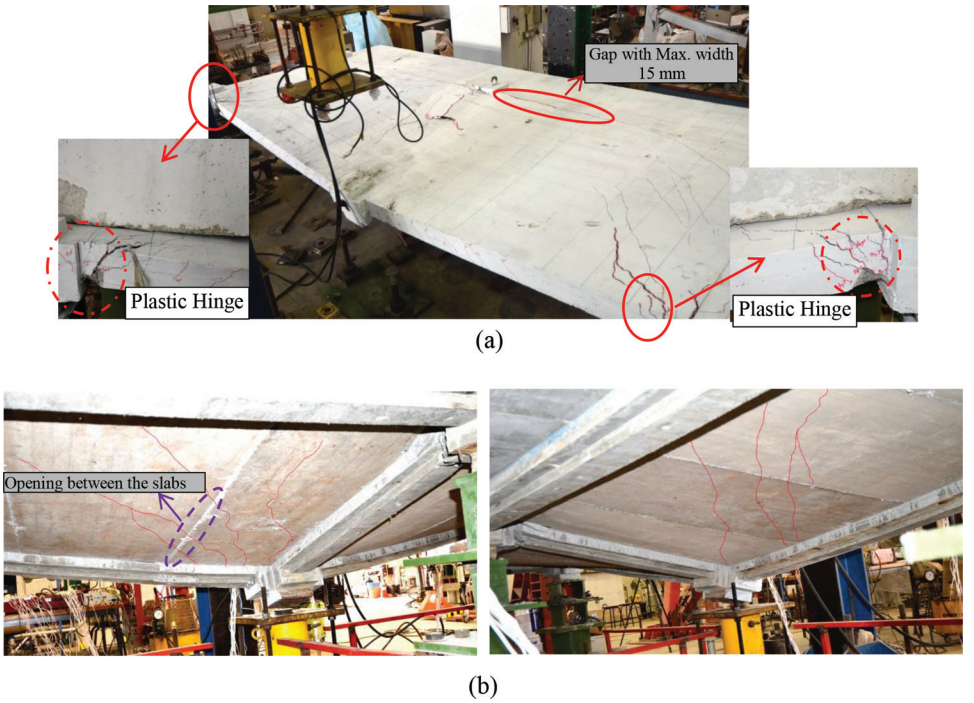

Fig. 8—Failure mode of Specimen PC1: (a) top view; and (b) bottom view.

–1.8 mm (–0.07 in.), which is attributed to the development of compressive arch action in Beam A1-A3 and compressive membrane action in the slab. When the vertical displacement exceeded 90 mm (3.5 in.), the outward movement begins to decrease. Inward movement is measured when the vertical displacement is over 246 mm (9.7 in.). The maximum inward movement is measured to 10 mm (0.39 in.) due to the development of catenary action and tensile membrane action. For PC1 and PC2, similar trends are observed. However, the maximum outward movements in PC1 and PC2 are –1.2 and –1.1 mm (–0.05 and –0.05 in.), respectively. The milder outward movement in the precast specimens may be due to less compressive arch action developed in precast beams. Different from RC1, the inward movements are observed in PC1 and PC2 when the vertical displacement reached approximately 300 mm (11.8 in.). Moreover, the maximum inward movement in PC1 and PC2 is 4.6 mm (0.18 in.) and 3.1 mm (0.12 in.), respectively. As the tensile membrane action for

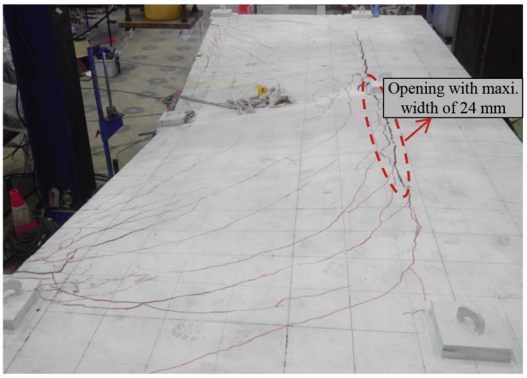

(a)

(b)

Fig. 9—Failure mode of Specimen PC2: (a) top view; and (b) bottom view.

precast specimen is mainly attributed into the welded wire reinforcement in the topping layer, larger vertical displacement is required to develop tensile membrane action and less inward movement is measured.

Strain gauge results

Figures 11 and 12 show the strain distribution in Beams A1-A3 and B2-A2 of Specimen RC1, respectively. As shown in Fig. 11, tensile strain is observed in top reinforcing bar near the side of Columns A1 and A3 and the bottom reinforcing bar near the center of Column A2. This is because of the bending moment reversal: the negative bending moment in beam end near to Column A2 before column removal changes to positive after removal of the column. The top reinforcing bar achieved tensile strength through the whole span in large deformation stage due to catenary action developed in the beam. As illustrated in Fig. 12, the Beam B2-A2 worked like cantilever beam during test and the first yielding of reinforcing bar occurred in the longitudinal reinforcing bar near Column B2. Figure 13 shows the strain distribution in Beam A1-A3 of PC2. As shown in the figure, the strain distribution is very similar to the control specimen, even in the large deformation stage. Thus, the integrity of the precast concrete frame with monolithic joints is well and it ensures the precast beams transfer the bending moment in the joints and to develop catenary action as well. For Specimen PC1, similar results are achieved. Figure 14 shows the strain distribution in the slab reinforcement of RC1, in the final of the test. Considerable tensile strain is observed in the top slab reinforcement near Columns A1 and B2, which indicated that the slab worked as flanges of the beams to provide flexural resistance. In comparison, the strain in the top reinforcement near Column B1 is quite milder, which coincides the failure mode of the specimen well (fewer

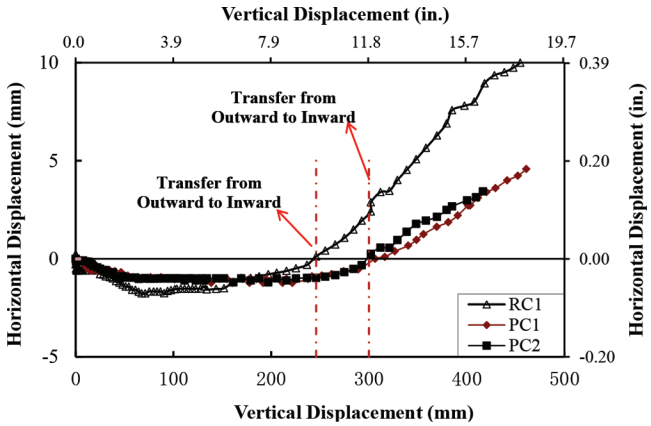

Fig. 10—Horizontal movement of Column A1.

cracks occurred in there). Similar to Qian et al.,[13] this is also due to less force redistributed into column B1 after removal of Column A2. For the strain value in the bottom reinforcing bar, it is observed that considerable tensile strain is also observed in the bottom reinforcing bar due to mobilization of tensile membrane action in slab. For precast specimens, only the strain distribution in the welded wire reinforcement is presented because the strain gauges are only installed there. As shown in Fig. 15(a), considerable tensile strain is only achieved in the welded wire reinforcement of PC1 nearby A1 and B2 due to the flexural action, but also in the middle width of the slab due to tensile membrane action. For PC2, similar results are observed, as shown in Fig. 15(b).

ANALYSIS AND DISCUSSION

To better understand the performance of PC frame-slab sub-assemblages to resist progressive collapse, and to quantify the effects of precast construction methodology on

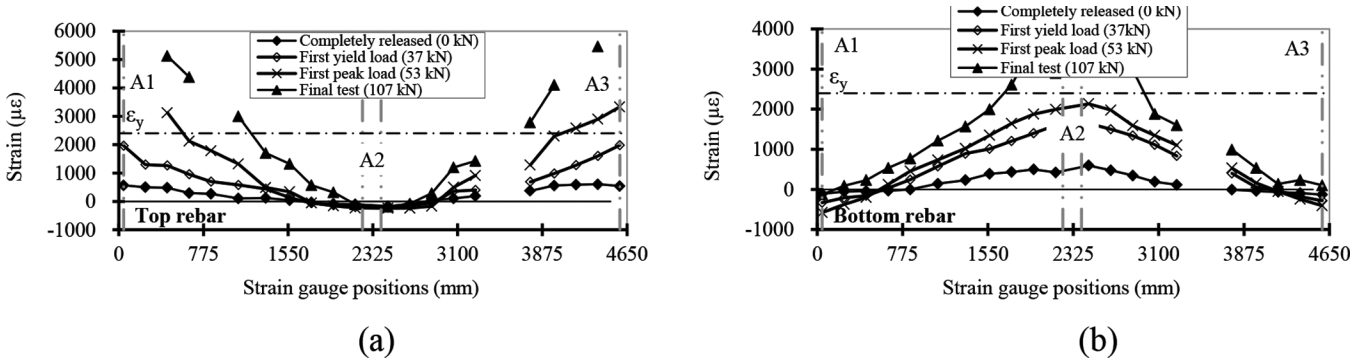

Fig. 11—Strain distribution in longitudinal reinforcing bar of Beam A1-A3 in RC1: (a) top; and (b) bottom.

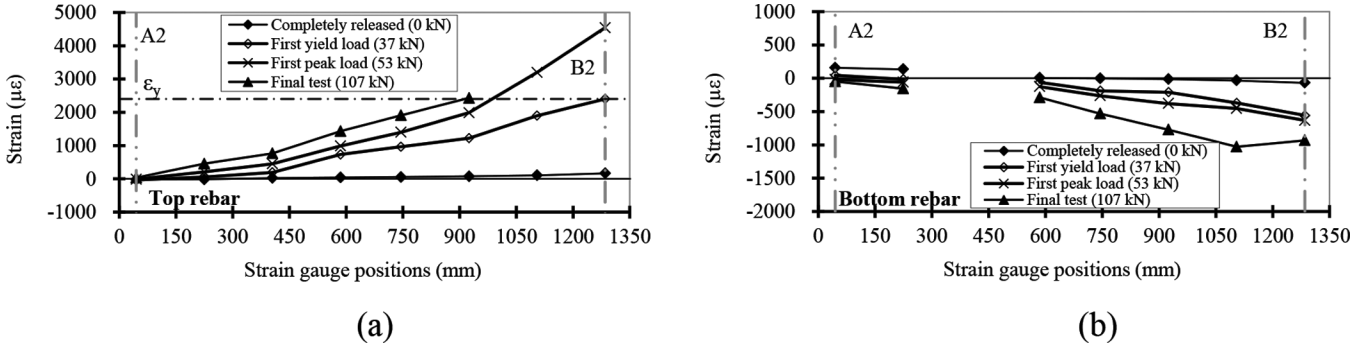

Fig. 12—Strain distribution in longitudinal reinforcing bar of Beam B1-B2 in RC1: (a) top; and (b) bottom.

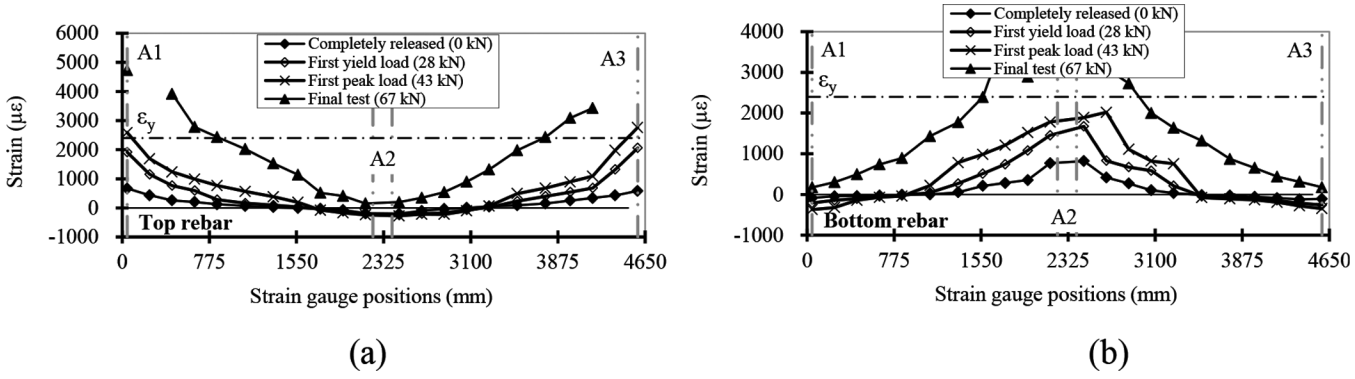

Fig. 13—Strain distribution in longitudinal reinforcing bar of Beam A1-A3 in PC2: (a) top; and (b) bottom.

progressive collapse resilience, a series of analysis is also carried out.

Dynamic strength of test specimens

Although the test program evaluated the effects of construction method on the quasi-static strength of RC buildings, it is necessary to conduct dynamic analysis to evaluate the impact of construction method on dynamic strength of the specimens as sudden column removal is more realistic. The energy-based capacity curve method is adopted to predict the dynamic strength of each specimen due to its high reliability and easy operation. Previous studies (Qian and Li[19] and Tsai[20]) have demonstrated the accuracy of capacity curve method and it is mathematically expressed as

$$P_{CC}(u_d) = \frac{1}{u_d}\int_0^{u_d} P_{NS}(u)du \quad (1)$$

where $P_{CC}(u)$ and $P_{NS}(u)$ represent the capacity function and the nonlinear static loading estimated at the displacement demand u, respectively.

Figure 16 illustrates the dynamic performance of tested specimens. As shown in the figure, the dynamic ultimate capacity of RC1, PC1, and PC2 are 96.8 kN (21.8 kip), 67.0 kN (15.1 kip), and 68.5 kN (15.4 kip), respectively. Thus, cast-in-place RC specimen increased the dynamic ultimate strength of PC specimen up by 44.4%. This is mainly because the cast-in-place RC slab could provide much higher yield strength and the ultimate strength in tensile membrane action stage.

Yield strength of test specimens

As the yield strength and corresponding initial stiffness are very critical for specimens to resist progressive collapse (the first defense line), yield-line method is adopted to predict their yield strength.

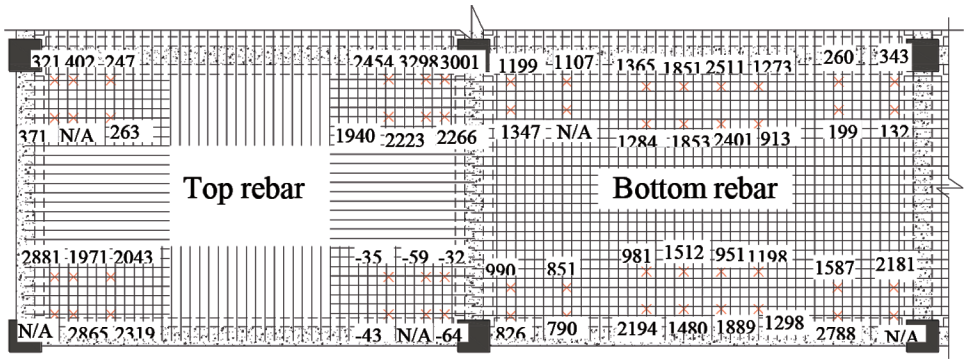

Fig. 14—Strain gauge results in slab reinforcement of Specimen RC1 at final test.

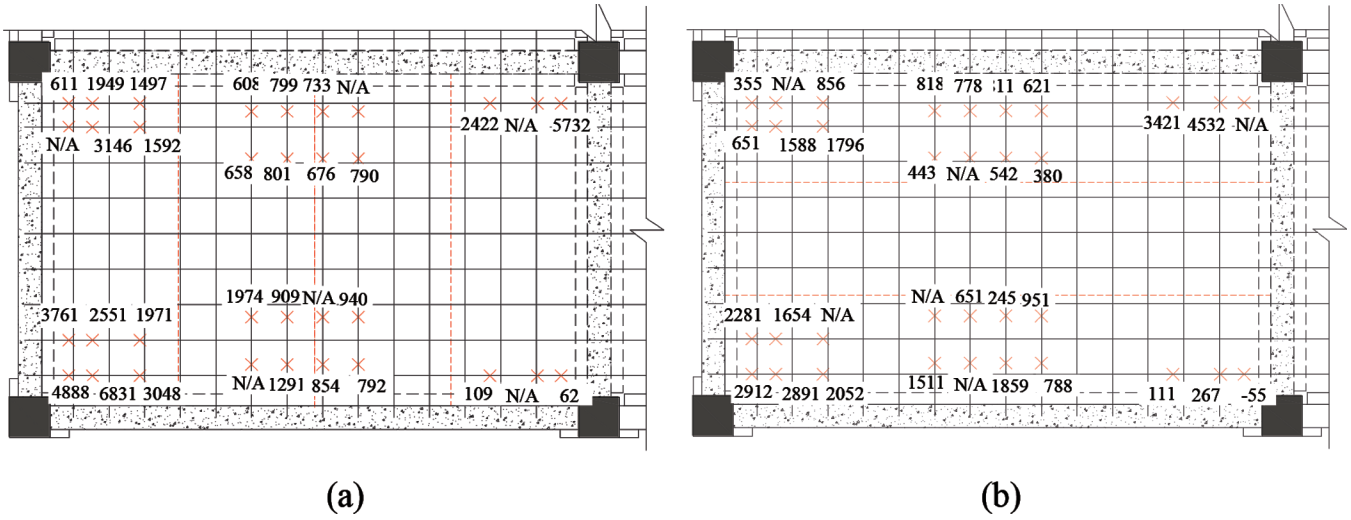

Fig. 15—Strain gauge results in slab reinforcement of precast specimens at final test: (a) PC1; and (b) PC2.

For RC1, as shown in Fig. 17, the internal virtual work due to rotation of plastic hinges in the beams and yield lines in the slab is

$$\sum W_I = m'_{sy}L_x\theta_y + 2m'_{sx}L_y\theta_x + 2m_{sx}L_y\theta_x + m_{sy}L_x\theta_y + 2M'_{PB}\theta_x + M'_{IB}\theta_y + 2M_{PB}\theta_x \quad (2)$$

where $L_x = 4.8$ and $L_y = 1.5$ are the total span of the slab in x and y directions; $\theta_x = 2\delta/L_x$ and $\theta_y = \delta/L_y$ are the rotations of yield lines or plastic hinges; M_{PB} and M_{PB}' are the positive and negative bending moment of the perimeter beam; δ is the vertical deflection at the lost exterior Column A2; M_{IB} and M_{IB}' are the positive and negative bending moment of the interior beam; m_{sx} and m_{sx}' are the positive and negative bending moment of the slab in the x direction; and m_{sy} and m_{sy}' are the positive and negative bending moment of the slab in y direction.

The bending moment of beams is calculated by

$$M_b = A_{bt}f_y\left(d_b - 0.59A_{bt}\frac{f_y}{f'_c \times b}\right) \quad (3)$$

where A_{bt} is the area of tensile reinforcement in beam section; f_y is yield strength of beam longitudinal reinforcement; f_c' is compressive strength of concrete; d_b is the beam effective depth; and b is the beam width. It should be noted that the flanges of slab, as suggested in ACI 318-11,[21] is included when determining the negative bending moment of the beams.

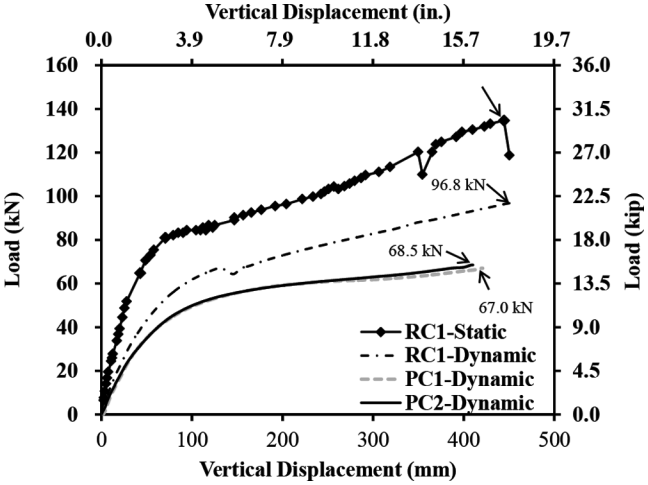

Fig. 16—Comparison of dynamic strength of test specimens.

The bending moment of slabs is calculated by

$$M_s = A_s f_y\left(d_s - 0.59A_s\frac{f_y}{f'_c}\right) \quad (4)$$

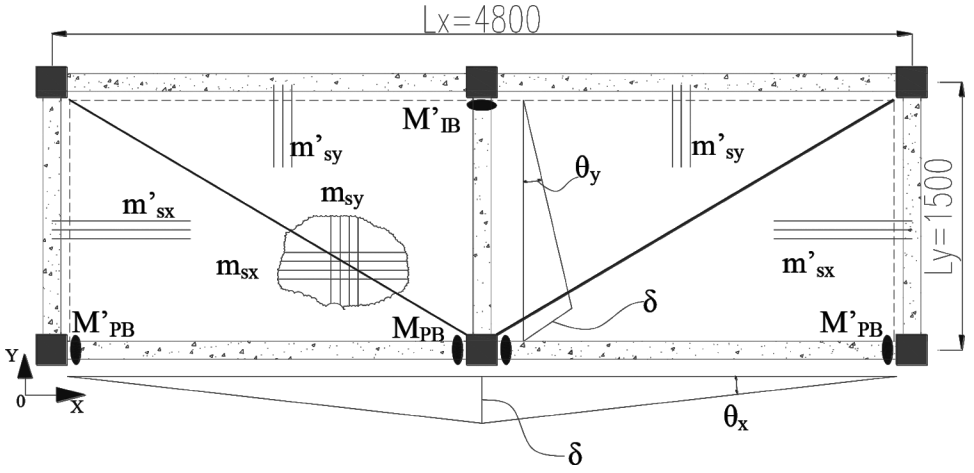

Fig. 17—Format of yield-line for test specimens.

where A_s is the tensile slab reinforcement per unit width; and d_s is the slab effective depth.

The external virtue work is

$$\sum W_E = 4 \times \frac{\delta}{3} \times \frac{1}{2} \times \frac{L_x}{2} \times L_y \times w_i + F_y \delta = \frac{\delta}{3} L_x L_y w_i + F_y \delta \quad (5)$$

where F_y is the theoretical yield load capacity.

Thus, the predicated additional axial force at yield stage of RC1 is 69 kN (15.5 kip), which is approximately 108% of the measured one. Thus, generally, the yield-line method could predict the yield strength of cast-in-place RC specimen well.

For precast specimens, as the scaled precast hollow core slabs are reinforced with non-prestressed reinforcing bar and no obvious incompatible behavior is observed between precast hollow core slab and cast-in-place topping layer, the positive bending moment of precast slabs are determined based on Eq. (4). However, as the reinforcements in precast hollow core slab are mainly reinforced in the longitudinal direction, only m_{sy} and m_{sx} are effective in PC1 and PC2, respectively. Thus, the internal work of PC1 and PC2 are determined by Eq. (6) and (7), respectively. The contribution of reinforcements in precast hollow slab could be included for determining m_{sy}' in PC1 and m_{sx}' in PC2, respectively

$$\begin{aligned} \sum W_I = {} & m'_{sy} L_x \theta_y + 2 m'_{sx} L_y \theta_x + m_{sy} L_x \theta_y \\ & + 2 M'_{PB} \theta_x + M'_{IB} \theta_y + 2 M_{PB} \theta_x \end{aligned} \quad (6)$$

$$\begin{aligned} \sum W_I = {} & m'_{sy} L_x \theta_y + 2 m'_{sx} L_y \theta_x + m_{sx} L_y \theta_x \\ & + 2 M'_{PB} \theta_x + M'_{IB} \theta_y + 2 M_{PB} \theta_x \end{aligned} \quad (7)$$

Based on Eq. (5) through (7), the predicted additional axial force in yield stage is 57 kN (12.8 kip) and 53 kN (11.9 kip), respectively. As the measured yield load is 51 kN (11.5 kip) and 50 kN (11.2 kip), respectively, the analytical results are approximately 112% and 106% of the test results correspondingly. Thus, in general, the analytical model is able to predict the yield load of test specimens well although the behavior of precast specimens is relatively complicated.

Tie-force method

The U. S. Department of Defense (DoD) design guideline[22] is a refined version of the old DoD guideline,[23] including plentiful improvements. One of the substantial revisions in the DoD[22] is that the horizontal tie forces (internal and peripheral) are no longer permitted to be contributed in the beams, girders, and spandrels (unless the designer can prove that these members are able to carry tensile loads while it undergoes large rotations; that is, 0.2 rad). As shown in Table 3, the required peripheral tie force is determined to 37.2 kN (8.4 kip) for test specimens in accordance with DoD[22] and Eq. (8)

$$F_r = 6 w_F L_1 L_p \quad (8)$$

where w_F is the floor load (8.6 kN/m^2 in current study); L_1 is the span of frame in the direction under consideration; and L_p equals 0.3 m for one-third-scale model.

As the chord rotation, which is defined as the ratio of vertical displacement to the design span length by the DoD,[22] of perimeter Beams A1-A2 or A2-A3 is less than 0.2 rad. Thus, the allowable peripheral tie force purely relied on the slab trip F_a is 18.1 kN (4.1 kip), 6.5 kN (1.5 kip), and 6.5 kN (1.5 kip) for RC1, PC1, and PC2, respectively. It should be noted that the tie force of RC specimen is determined based on the continuous bottom reinforcement while the tie force of PC specimen is calculated based on the continuous welded wire reinforcement in the topping layer. Thus, based on the tie-force provision in existing DoD design guideline,[22] the designed RC and PC specimens did not satisfy the requirements of peripheral tie force. However, based on the measured ultimate load capacity, the measured tie force is 135 kN (30.3 kip), 91 kN (20.4 kip), and 94 kN (21.1 kip), respectively, which is much larger than the tie-force requirement. The main cause of the contradiction is that one ignored the tie force contribution from the peripheral Beams A1-A2, A2-A3 as their rotation is less than 0.2 rad. As tabulated in Table 3, the peripheral beams could provide tie force as large as 83.3 kN (18.7 kip). Thus, it is necessary to re-evaluate the reliability of the rotation requirements (0.2 rad) for the beams to contribute tie force whichever cast-in-place or precast concrete frames.

Table 3—Comparison of measured tie force with required tie force determined based on DoD[23]

Test	RTS, kN (kip)	ATS, kN (kip)	ATB, kN (kip)	MT, kN (kip)
RC1	37.2 (8.4)	18.1 (4.1)	83.3 (18.7)	135 (30.4)
PC1	37.2 (8.4)	6.5 (1.5)	83.3 (18.7)	91 (20.4)
PC2	37.2 (8.4)	6.5 (1.5)	83.3 (18.7)	94 (21.1)

Notes: RTS is required tie force; ATS is allowable tie force from slab; ATB is allowable tie force from beams; MT is measured tie force.

Effects of precast construction methodology

As shown in Table 2, the measured yield strength, first peak strength, and ultimate strength of RC1 is 64 kN (14.4 kip), 81 kN (18.2 kip), and 135 kN (30.3 kip), respectively. Thus, the compressive arch action and compressive membrane action could increase the yield strength by 26.6%. Meanwhile, the catenary action and tensile membrane action could increase the yield strength by 111%. However, for PC1, its yield strength, first peak strength, and ultimate strength are 51 kN (11.5 kip), 68 kN (15.3), and 94 kN (21.1 kip), respectively. Thus, the compressive arch action developed in PC beam and compressive membrane action developed in PC slab system could increase the yield strength by 33.3%. Meanwhile, the catenary action developed in PC beam and tensile membrane action developed in PC slab system could increase the yield strength by 84.3%. Thus, precast construction methodologies will not detrimentally affect the development of compressive arch action in PC beam and compressive membrane action in PC slab system. However, as shown in Fig. 18, the PC slab is discontinuous from the bottom view and only welded wire reinforcement in the topping layer could contribute tensile membrane action in large deformation stage, less benefits from tensile membrane action in PC specimens. Comparing the behavior of PC2 to PC1 indicated that the layout of PC slab has little effects on the performance of PC buildings to resist progressive collapse although the locations of the openings between the PC slab and surrounding beam may quite different.

CONCLUSIONS

The experimental study conducted in this research has derived the following conclusions:

1. The failure mode of cast-in-place specimens indicated that the plastic hinge is first deformed in the interior Beam A2-B2, which is worked as cantilever beam during test. The shear failure occurred in the corner joint (Column A1) in the large deformation stage, which may hamper the development of catenary action in perimeter Beam A1-A2 and A2-A3. The failure mode of precast specimens indicated that initial crack pattern in precast specimens is similar to the cast-in-place specimen. The cracks in the bottom of the slab are continuous; even the precast slabs are tiled and discontinuous. However, in large deformations stage (stage of catenary action and tensile membrane action), substantial openings will occur in between the precast cast slabs and the interfaces between the precast slab and surrounding beams.

2. The yield line of precast slab with topping layer is similar to that of cast-in-place slab. The analytical results indicated that yield-line method could well predict the yield load of tested specimens, which were controlled by flexural failure. The load-resisting functions and strain gauge results indicated that compressive arch action and catenary action could effectively develop in PC beam when monolithic joint and welding connection is used to continue the beam longitudinal reinforcement. Moreover, similar to cast-in-place frames, considerable compressive membrane action could develop in the PC slab system. However, different to cast-in-place frames, less tensile membrane action is able to develop in PC slab system as the main tensile stress is developed in the welded wire reinforcement in the topping layer.

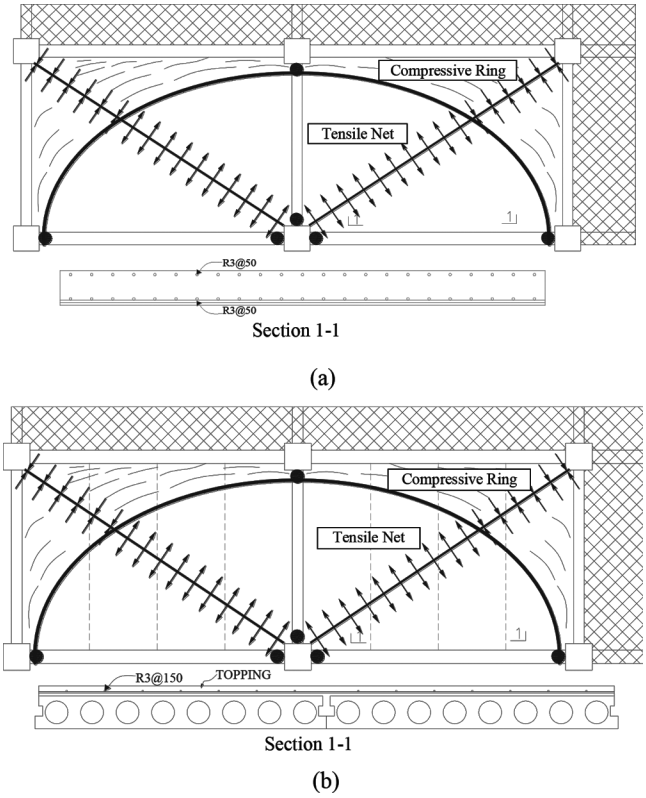

Fig. 18—Internal force in panels of test specimens: (a) RC1; and (b) PC1.

3. Evaluating the reliability of the tie force method proposed in the existing design guideline indicated that existing provisions for tie force method may achieve conservative results, especially for the peripheral horizontal tie, which is because existing provision tends to provide tensile force in slab rather than the beams. However, the test results had indicated that both cast-in-place or precast perimeter beams could provide major horizontal tie force, which should not be ignored even if their rotation capacity is less than 0.2 rad.

AUTHOR BIOS

ACI member **Kai Qian** *is a Professor in the College of Civil Engineering and Architecture, Guilin University of Technology, Guilin, China. He received his MSC and PhD from Nanyang Technological University, Singapore. His research interests include reinforced concrete and prestressed concrete structure design, particularly in the area of progressive collapse and blast resistance of building structures.*

ACI member **Bing Li** *is an Associate Professor in the School of Civil and Environmental Engineering at Nanyang Technological University. He received his PhD from the University of Canterbury, Christchurch, New*

Zealand. He is a member of ACI Committee 377, Performance-Based Structural Integrity and Resilience of Concrete Structures, and Joint ACI-ASCE Committees 352, Joints and Connections in Monolithic Concrete Structures, and 441, Reinforced Concrete Columns.

REFERENCES

1. Marjanishvili, S., and Agnew, E., "Comparison of Various Procedures for Progressive Collapse Analysis," *Journal of Performance of Constructed Facilities*, ASCE, V. 20, No. 4, 2006, pp. 365-374. doi: 10.1061/(ASCE)0887-3828(2006)20:4(365)

2. Mohamed, O. A., "Progressive Collapse of Structures: Annotated Bibliography and Comparison of Codes and Standards," *Journal of Performance of Constructed Facilities*, ASCE, V. 20, No. 4, 2006, pp. 418-425. doi: 10.1061/(ASCE)0887-3828(2006)20:4(418)

3. Ruth, P.; Marchand, K. A.; and Williamson, E. B., "Static Equivalency in Progressive Collapse Alternate Path Analysis: Reducing Conservatism while Retaining Structural Integrity," *Journal of Performance of Constructed Facilities*, ASCE, V. 20, No. 4, 2006, pp. 349-364. doi: 10.1061/(ASCE)0887-3828(2006)20:4(349)

4. Sasani, M.; Bazan, M.; and Sagiroglu, S., "Experimental and Analytical Progressive Collapse Evaluation of Actual Reinforced Concrete Structure," *ACI Structural Journal*, V. 104, No. 6, Nov.-Dec. 2007, pp. 731-739.

5. Sasani, M., "Response of a Reinforced Concrete Infilled-Frame Structure to Removal of Two Adjacent Columns," *Engineering Structures*, V. 30, No. 9, 2008, pp. 2478-2491. doi: 10.1016/j.engstruct.2008.01.019

6. Yi, W.; He, Q.; Xiao, Y.; and Kunnath, S. K., "Experimental Study on Progressive Collapse-Resistant Behavior of Reinforced Concrete Frame Structures," *ACI Structural Journal*, V. 105, No. 4, July-Aug. 2008, pp. 433-439.

7. Su, Y. P.; Tian, Y.; and Song, X. S., "Progressive Collapse Resistance of Axially-Restrained Frame Beams," *ACI Structural Journal*, V. 106, No. 5, July-Aug. 2009, pp. 600-607.

8. Tsai, M. H., "An Analytical Methodology for the Dynamic Amplification Factor in Progressive Collapse Evaluation of Building Structures," *Mechanics Research Communications*, V. 37, No. 1, 2010, pp. 61-66. doi: 10.1016/j.mechrescom.2009.11.001

9. Kai, Q., and Li, B., "Dynamic Performance of RC Beam-Column Substructures under the Scenario of the Loss of a Corner Column-Experimental Results," *Engineering Structures*, V. 42, 2012, pp. 154-167. doi: 10.1016/j.engstruct.2012.04.016

10. Qian, K., and Li, B., "Slab Effects on the Response of Reinforced Concrete Substructures after Loss of Corner Column," *ACI Structural Journal*, V. 109, No. 6, Nov.-Dec. 2012, pp. 845-855.

11. Dat, P. X., and Tan, K. H., "Experimental Study of Beam-Slab Substructures Subjected to a Penultimate-Internal Column Loss," *Engineering Structures*, V. 55, 2013, pp. 2-15. doi: 10.1016/j.engstruct.2013.03.026

12. Yu, J.; Rinder, T.; Stolz, A.; Tan, K.; and Riedel, W., "Dynamic Progressive Collapse of an RC Assemblage Induced by Contact Detonation," *Journal of Structural Engineering*, ASCE, V. 140, No. 6, 2014, p. 04014014 doi: 10.1061/(ASCE)ST.1943-541X.0000959

13. Qian, K.; Li, B.; and Ma, J. X., "Load-Carrying Mechanism to Resist Progressive Collapse of RC Buildings," *Journal of Structural Engineering*, ASCE, V. 141, No. 2, 2015, p. 04014107 doi: 10.1061/(ASCE)ST.1943-541X.0001046

14. Lew, H. S.; Bao, Y. H.; Pujol, S.; and Sozen, M. A., "Experimental Study of Reinforced Concrete Assemblies under Column Removal Scenario," *ACI Structural Journal*, V. 111, No. 4, July-Aug. 2014, pp. 881-892. doi: 10.14359/51686739

15. Main, J. A.; Bao, Y. H.; Lew, H. S.; and Sadek, F., "Robustness of Precast Concrete Frames: Experimental and Computational Studies," *Structures Congress*, 2014, pp. 2210-2220.

16. Qian, K., and Li, B., "Performance of Precast Concrete Substructures with Dry Connections to Resist Progressive Collapse," *Journal of Performance of Constructed Facilities*, ASCE, V. 32, No. 2, 2018, p. 04018005. doi: 10.1061/(ASCE)CF.1943-5509.0001147

17. Park, R., "A Perspective on the Seismic Design of Precast Concrete Structures in New Zealand," *PCI Journal*, V. 40, No. 3, 1995, pp. 40-60. doi: 10.15554/pcij.05011995.40.60

18. Xue, W., and Yang, X., "Seismic Tests of Precast Concrete Moment Resisting Frames and Connections," *PCI Journal*, V. 55, No. 3, 2010, pp. 102-121. doi: 10.15554/pcij.06012010.102.121

19. Qian, K., and Li, B., "Dynamic Disproportionate Collapse in Flat-Slab Structures," *Journal of Performance of Constructed Facilities*, ASCE, V. 29, No. 5, 2015, p. B4014005. doi: 10.1061/(ASCE)CF.1943-5509.0000680

20. Tsai, M. H., "An Analytical Methodology for the Dynamic Amplification Factor in Progressive Collapse Evaluation of Building Structures," *Mechanics Research Communications*, V. 37, No. 1, 2010, pp. 61-66. doi: 10.1016/j.mechrescom.2009.11.001

21. ACI Committee 318, "Building Code Requirements for Structural Concrete (ACI 318-11) and Commentary (ACI 318R-11)," American Concrete Institute, Farmington Hills, MI, 2011, 433 pp.

22. DoD, "Design of Building to Resist Progressive Collapse," *Unified Facility Criteria*, UFC 4-023-03, U.S. Department of Defense, Washington, DC, 2009.

23. DoD, "Design of Building to Resist Progressive Collapse" *Unified Facility Criteria*, UFC 4-023-03, U.S. Department of Defense, Washington, DC, 2005.